

Ground-State Shapes and Structures of Colloidal Domains

Jianlan Wu and Jianshu Cao*

*Department of Chemistry,
Massachusetts Institute of Technology
Cambridge, MA 02139*

(Dated: First submitted August 21, 2004)

Abstract

In charged colloidal suspensions, the competition between square-well attraction and long-range Yukawa repulsion leads to various stable domains and Wigner supercrystals. Using a continuum model and symmetry arguments, a phase diagram of spheres, cylinders, and lamellae is obtained as a function of two control parameters, the volume fraction and the ratio between the surface tension and repulsion. Above a critical value of the ratio, the microphase cannot be supported by the Yukawa repulsion and macroscopic phase separation occurs. This finding quantitatively explains the lack of pattern formation in simple liquids because of the small hard sphere diameter in comparison with the size of macromolecules. The phase diagram also predicts microphase separation at zero value of the ratio, suggesting the possibility of self-assembly in repulsive systems.

PACS numbers: 82.70.Dd, 05.65.+b, 64.70.-p

* Email: jjianshu@mit.edu

Microphase separation is ubiquitous in soft matter systems[1, 2, 3, 4, 5, 6, 7, 8]. For example, microphase separation in block copolymers results from mixing of two or more chemically different polymer segments[3]. Competition of hydrophobic and hydrophilic head-groups of amphiphiles leads to micelles in the water solution[4]. The self-assembly processes in charged colloidal suspensions and protein solutions can lead to the formation of stable domains and Wigner supercrystals (see Fig. 1) at low temperatures. The investigation of charged colloids and protein solutions is particularly interesting because they can be approximated as one-component systems with an effective isotropic pairwise interaction after averaging out the degrees of freedom of dispersing medium. This effective interaction is composed of a hard-core potential, a long-range electrostatic repulsion, and a short-range attraction. The screened Coulomb repulsion is described by a Yukawa potential[9, 10]. Since more complicated potential forms qualitatively lead to the same phenomena[11, 12], for simplicity, we model the short-range attraction by a square-well potential. The overall pairwise interaction between two colloidal particles separated by r is given by

$$u(r) = \begin{cases} \infty & r \leq \sigma \\ -\varepsilon & \sigma < r \leq \lambda\sigma \\ u_Y(r) = A\zeta r^{-1}e^{-r/\zeta} & r > \lambda\sigma \end{cases}, \quad (1)$$

where σ is the colloidal diameter. The attraction depth ε and repulsion strength A are temperature dependent, and ε is usually greater than the average thermal fluctuation. For convenience all the length variables in this letter are dimensionless in units of the screening length ζ . The pairwise and isotropic interaction in Eq. (1) represents one of the simplest self-assembly systems that can be studied explicitly.

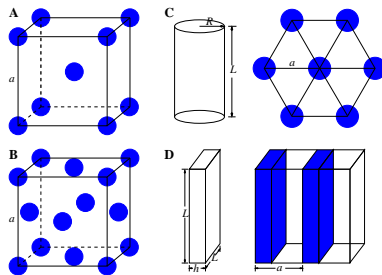


FIG. 1: Super structures of domains: A) bcc lattice of spherical domains, B) fcc lattice of spherical domains, C) a cylindrical domain and the resulting 2D triangular lattice, D) a lamellar domain and the resulting 1D lattice.

At low temperatures, shapes and sizes of colloidal domains are narrowly distributed, and their arrangements in space are highly ordered. A perfect superlattice composed of identical colloidal domains is an ideal reference (ground) state. In this letter we concentrate on domain patterns in the ground state. Entropic effects induced by thermal fluctuations will be studied elsewhere. Without thermal effects, we determine the most stable (optimal) shape, size, and superlattice (see Fig. 1) for ground-state domain patterns by globally minimizing the energy density. At low temperatures, this evaluation is simplified by a continuum approximation: Colloidal particles are closely packed inside a domain and the characteristic domain size is much larger than the particle size. Similar models have been used in the study of two-dimensional (2D) lipid domains[2]. In our continuum model, the short-range attraction gives rise to bulk adhesion and surface energy. The density of the adhesive energy is a constant in the leading order for a given colloidal number density ρ or equivalently a given volume fraction, $\phi = \pi\rho\sigma^3/6$. The bulk adhesion does not affect the domain shapes and is not included in this letter. For a domain with area S , the surface energy is $U_S = \gamma S$, where the surface tension γ is proportional to the attraction depth ϵ in the lowest order approximation. Throughout this letter, γ is assumed to be independent of domain shapes. The sum of the long-range Yukawa potential is separated into two parts,

$$\begin{aligned}
\sum_{i<j} u_Y(r_{ij}) &= \sum_{m=1}^{N_d} U_Y^{(1)}(m) + \sum_{m<n}^{N_d} U_Y^{(2)}(m, n) \\
&= \sum_{m=1}^{N_d} \frac{\rho_1^2}{2} \int_{v_{d,m}} d\vec{r}_1 \int_{v_{d,m}} d\vec{r}_2 u_Y(r_{12}) \\
&\quad + \sum_{m<n}^{N_d} \rho_1^2 \int_{v_{d,m}} d\vec{r}_1 \int_{v_{d,n}} d\vec{r}_2 u_Y(r_{12}), \tag{2}
\end{aligned}$$

where $U_Y^{(1)}(m)$ is the intra-domain repulsion for domain m , $U_Y^{(2)}(m, n)$ is the inter-domain repulsion between domains m and n , and N_d is the total number of domains. Here ρ_1 is the colloidal number density within domains and larger than the overall number density ρ . The self energy of a single domain is the sum of the intra-domain repulsion and the surface energy, $E_1 = U_S + U_Y^{(1)}$. The sum of the inter-domain repulsions results in the lattice energy, $U_L = (1/2) \sum_{n(\neq 1)}^{N_d} U_Y^{(2)}(1, n)$. In the ground state, all the domains in one phase are identical so that the energy of each domain is given by $E_{\text{tot}} = E_1 + U_L$. In our continuum model, the morphologies of domain patterns are thus determined by minimizing E_{tot}/v_d , where v_d is the domain volume.

We now apply the continuum model to study various domain patterns shown in Fig. 1. Spheres have the smallest surface energy and highest spatial symmetry. For a spherical domain with radius R , the intra-domain Yukawa contribution $U_Y^{(1)}$ is simplified using the Fourier transform technique. The summation of the surface energy U_S and the intra-domain repulsion $U_Y^{(1)}$ results in the self energy of a spherical domain,

$$E_1 = \frac{E_0}{R^3} [2R^3 + 3(\alpha - 1)R^2 + 3 - 3(1 + R)^2 e^{-2R}], \quad (3)$$

where $E_0 = v_d \varepsilon_0$ arises from a constant energy density $\varepsilon_0 = \pi \rho_1^2 A \zeta^3$ and the domain volume $v_d = 4\pi R^3/3$. As shown in Eq. (3), the competition between the surface tension and the Yukawa repulsion is described by a single control parameter, $\alpha = \gamma/\pi \rho_1^2 A \zeta^4$. In the low density limit, domains are far apart from one another so that an individual domain can be treated as an isolated system and the lattice energy can be neglected. The self energy has a minimum at a finite radius for $\alpha < 1$, whereas E_1 is a monotonously decreasing function of R for $\alpha \geq 1$. Thus $\alpha_c = 1$ is a critical point: Spherical domains with finite sizes are stable for $\alpha < \alpha_c$, whereas the phase separation occurs for $\alpha \geq \alpha_c$. The self energy minimum $E_{1,m}$ and the associated radius R_m are plotted in Fig. 2. In the limit of strong repulsion ($\alpha \rightarrow 0$), we obtain two asymptotic forms, $R_m \sim \sqrt[3]{15\alpha}/2$ and $E_{1,m}/E_0 \sim 3\sqrt[3]{3\alpha^2/5}$. The size of the spherical domain grows as α increases. In the phase separation limit ($\alpha \rightarrow \alpha_c^-$), the stable radius and energy minimum are asymptotically given by $R_m \sim \sqrt{3}(1 - \alpha/\alpha_c)^{-1/2}$ and $E_{1,m}/E_0 \sim 2[1 - (1 - \alpha/\alpha_c)^{3/2}/\sqrt{3}]$, respectively. These asymptotic relations can be tested experimentally.

For a finite density (volume fraction), the balance of the self energy E_1 and the lattice energy U_L from inter-domain repulsions leads to a 3D supercrystal, e.g., body centered cubic (bcc) and face centered cubic (fcc) lattices of spheres (see Fig. 1A and B). The lattice energy U_L depends on the inter-domain repulsion and the lattice structure. Using the spherical harmonic expansion method, the inter-domain repulsion between two spheres separated by r is derived as

$$U_Y^{(2)}(r) = \frac{3E_0}{R^3} [(R+1)e^{-R} + (R-1)e^R]^2 \frac{e^{-r}}{r}. \quad (4)$$

The spatial periodicity of a Wigner lattice is related to the volume fraction. For example, the lengths of primitive cells for bcc and fcc lattices (see Fig. 1A and B) are given by $a = \eta\phi^{-1/3}R$, where we have $\eta_{\text{fcc}} = (16\pi/3)^{1/3}$ for the fcc lattice, and $\eta_{\text{bcc}} = (8\pi/3)^{1/3}$ for

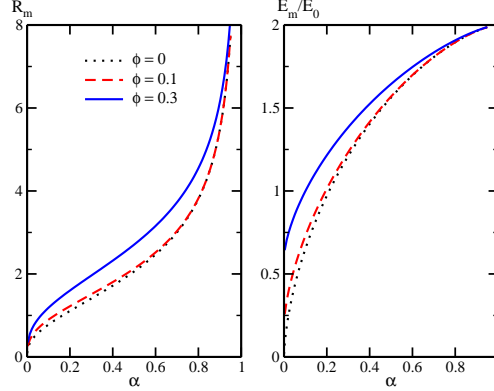


FIG. 2: The optimal radius R_m and the energy minimum $E_{1,m}$ ($E_{\text{tot},m}$) of a spherical domain in the isolated case (dotted lines) and in fcc lattices at finite volume fractions, where the dashed lines are for $\phi = 0.1$ and the solid lines are for $\phi = 0.3$.

the bcc lattice. Using the spatial periodicity, we sum the inter-domain repulsions of the fcc (bcc) lattice and obtain the lattice energy as

$$U_L = \frac{3E_0\phi^{1/3}}{\eta R^4} [(R+1)e^{-R} + (R-1)e^R]^2 \times \sum_{\vec{n} \neq 0} \frac{\exp(-\eta\phi^{-1/3}Rx_{\vec{n}}/2)}{x_{\vec{n}}}. \quad (5)$$

The reduced distance $x_{\vec{n}}$ in the above equation is given by $x_{\vec{n}} = [2(n_1^2 + n_2^2 + n_3^2 + n_1n_2 + n_2n_3 + n_3n_1)]^{1/2}$ for the fcc lattice, and $x_{\vec{n}} = [3(n_1^2 + n_2^2 + n_3^2) - 2(n_1n_2 + n_2n_3 + n_3n_1)]^{1/2}$ for the bcc lattice, where n_i can be any integers except for that all the n_i are zero. The total energy of a domain is the sum of the self energy in Eq. (3) and the lattice energy in Eq. (5). Minimization of the energy density for a given lattice using $\partial_R(E_{\text{tot}}/E_0) = 0$ leads to the stable radius R_m . Figure 2 shows that both R_m and the energy minimum $E_{\text{tot},m}$ increase with the volume fraction. By examining the subtle difference ($\sim 10^{-4}$) of $E_{\text{tot},m}$ between fcc and bcc lattices, we obtain the phase diagram displayed in Fig. 3. It demonstrates that the fcc lattice is usually more stable than the bcc lattice except for small values of α . Our results extend the previous studies on the fcc-bcc transition in Wigner particle solids with the Yukawa potential[13].

Dispersing medium surrounded by colloidal particles can be considered as cavities. For $\phi > 0.5$, cavities are dispersed in the sea of colloidal particles so that various shapes and structures of cavities can form in the same way as domains. The intrinsic mirror symmetry between conjugate colloidal domains and cavities requires that the optimal shape and

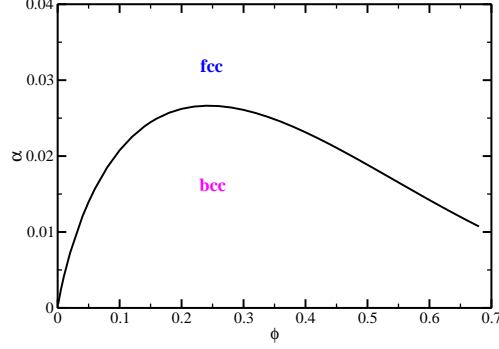


FIG. 3: The phase diagram for fcc and bcc supercrystals composed by spherical domains.

structure of cavities at $\phi(> 0.5)$ are the same as those of colloidal domains at $1 - \phi$. As a result, the cavity phase and the domain phase must be equivalent at $\phi = 0.5$, which can be achieved by the lamellar shape and its topological variations. Following the same domain-cavity symmetry argument, lamellae are expected to be preferred in the phase separation limit ($\alpha \rightarrow \alpha_c^-$).

Next we investigate lamellar domains. For a lamellar domain with a finite width h , and infinite length and height ($L \rightarrow \infty$), its surface energy is given by $U_s = 2\gamma(L^2 + 2Lh) \approx 2E_0\alpha h^{-1}$, where $E_0 = v_d\varepsilon_0 = L^2h\varepsilon_0$. Following Eq. (2), we obtain the intra-domain repulsive energy,

$$U_Y^{(1)} = 2E_0h^{-1} [h - 1 + e^{-h}]. \quad (6)$$

In the ground state, all lamellar domains are parallel and form a one-dimensional supercrystal (see Fig. 1D). To obtain the lattice energy, we calculate the repulsion energy between two parallel lamellar domains separated by r ,

$$U_Y^{(2)}(r) = 2E_0h^{-1}e^{-r}(e^h + e^{-h} - 2). \quad (7)$$

At the volume fraction ϕ , the distance between two arbitrary lamellar domains is given by $|n|\phi^{-1}h$, where n is a nonzero integer. The lattice energy for each lamellar domain is given by

$$\begin{aligned} U_L &= E_0h^{-1} (e^h + e^{-h} - 2) \sum_{n \neq 0} e^{-|n|\phi^{-1}h} \\ &= 2E_0 \frac{e^h + e^{-h} - 2}{h(e^{h/\phi} - 1)}. \end{aligned} \quad (8)$$

We determine the optimal width h_m from minimization of E_{tot}/E_0 . Similar to spherical domains, lamellar domains with a finite width can exist only for $\alpha < \alpha_c$. In the limit of strong repulsion ($\alpha \rightarrow 0$) at a finite volume fraction, the lamellar width and the total energy are asymptotically given by $h_m \sim \sqrt[3]{6\phi\alpha/(1-\phi)^2}$ and $E_{\text{tot,m}}/E_0 = 2\phi + \sqrt[3]{9(1-\phi)^2\alpha^2/(2\phi)}$, respectively. By comparing $E_{\text{tot,m}}$ of spheres and lamellae, we obtain their relative stability, as shown in Fig. 4. As expected, lamellar shapes are more stable than spheres when α approaches the critical value α_c , or when the volume fraction approaches 0.5.

The spatial symmetry of spheres is the highest and that of lamellae is the lowest. It is natural to speculate that intermediate phases exist between these two limiting structures. One typical example is the 2D triangular lattice formed by cylindrical domains with the azimuthal symmetry (see Fig. 1C). For a cylindrical domain with a finite radius R and the infinite height ($L \rightarrow \infty$), the surface energy is given by $U_s = \gamma(2\pi R^2 + 2\pi RL) \approx 2E_0\alpha R^{-1}$ where $E_0 = v_d\varepsilon_0 = \pi R^2 L\varepsilon_0$. The intra-domain repulsion is derived from the Neumann addition theorem as

$$U_Y^{(1)} = 2E_0 [1 - 2I_1(R)K_1(R)], \quad (9)$$

where $I_n(x)$ and $K_n(x)$ are the modified Bessel functions of the first and second kinds, respectively. In this letter we consider the triangular lattice, although other lattice structures or mixed structures are also possible[3]. We apply the Neumann addition theorem to calculate the effective repulsion between two domains separated by r as

$$U_Y^{(2)}(r) = 8E_0 [I_1(R)]^2 K_0(r). \quad (10)$$

The length of the primitive equilateral triangle shown in Fig. 1C is related to the volume fraction as $a = (2\pi/\sqrt{3}\phi)^{1/2}R$. Using this relation, we calculate the lattice energy U_L from the lattice summation of the inter-domain repulsion. By solving $\partial_R(E_{\text{tot}}/E_0) = 0$, we obtain the optimal radius R_m and the energy minimum $E_{\text{tot,m}}$. Similar to other shapes, cylindrical domains are stable for $\alpha < \alpha_c$.

Comparing $E_{\text{tot,m}}$ calculated from different shapes and structures yields the global energy minimum and thus the optimal ground-state domain morphology. The central result of this letter is the phase diagram in Fig. 4, which describes the shape transformation between spherical, cylindrical, and lamellar domains. The ratio α between the surface tension and repulsion, and the volume fraction ϕ , are the two control parameters. Finite size domains

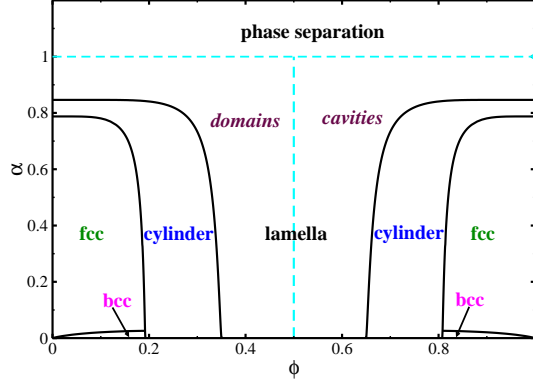


FIG. 4: A phase diagram for spherical, cylindrical, and lamellar shapes. The optimal structure formed by cavities for $\phi > 0.5$ is the mirror of that by colloidal domains at $1 - \phi$.

can be stabilized for $\alpha < \alpha_c = 1$, whereas phase separation is observed for $\alpha \geq \alpha_c$. Domain patterns stabilized in the small attraction limit ($\alpha \rightarrow 0$) suggest the possibility of self-assembly processes in repulsive systems[14]. The basic features of shape transformation are consistent with symmetry arguments. In the low density limit ($\phi \rightarrow 0$), spheres are preferred at small values of α , whereas lamellae are preferred as the system approaches phase separation. At larger volume fractions, structures in low dimensions (2D and 1D) become increasingly more stable. Spheres are unstable for $\phi > 0.19$, while cylinders are unstable for $\phi > 0.35$. At the equal volume fraction of colloidal domains and cavities ($\phi = 0.5$), only the lamellar phase is stable. The mirror symmetry between domains and cavities is used to produce the right half of the phase diagram for $\phi > 0.5$. The cylindrical regime completely separates spherical and lamellar regimes, demonstrating that 3D spheres undergo a transformation to 1D lamellae via 2D phases. Although we only compute cylinders, other intermediate shapes may exist.

In this letter we predict the shape transformation (see Fig. 4) of colloidal domain patterns in the ground state. Our study presents a simple and exactly solvable model system for understanding self-assembling phenomena based on a pairwise and isotropic potential. Ground-state domain patterns do not incorporate entropic effects induced by thermal fluctuations at finite temperatures. Temperature effects can be partially included in the current model by introducing the temperature-dependent surface tension $\gamma(T)$ and domain density $\rho_1(T)$. At higher temperatures, a more systematic treatment should involve the calculation of interphase free energies, where the distribution of shapes and distortion of structures are

accounted. Along this direction, the stability of domains with small distortions, the liquid-solid transition of particles within spherical clusters, and the formation of stable clusters at finite temperature are under investigation[15].

This work is supported by the NSF Career Award (Che-0093210) and the US Army through the Institute of Solidier Nano-technologies at MIT.

-
- [1] M. Seul and D. Andelman, *Science* **267**, 476 (1995).
 - [2] H. M. McConnell and V. T. Moy, *J. Phys. Chem.* **92**, 4520 (1988); H. M. McConnell, *Ann. Rev. Phys. Chem.* **42**, 171 (1991); J. M. Deutch and F. E. Low, *J. Phys. Chem.* **96**, 7097 (1992).
 - [3] L. Leibler, *Macromolecules* **13**, 1602 (1980); T. Ohta and K. Kawasaki, *Macromolecules* **19**, 2621 (1986); G. H. Fredrickson and E. Helfand, *J. Chem. Phys.* **87**, 697 (1987); M. Muthukumar *Macromolecules* **26**, 5259 (1993); M. W. Matsen and M. Schick, *Phys. Rev. Lett.* **72**, 2660 (1994).
 - [4] D. Blankschtein, G. M. Thurston, and G. B. Benedek, *Phys. Rev. Lett.* **54**, 955 (1985); A. Shiloach and D. Blankschtein, *Langmuir* **14**, 7166 (1998); L. Maibaum, A. R. Dinner, and D. Chandler, *J. Phys. Chem. B* **108**, 6778 (2004); S. Tsonchev, G. C. Schatz, and M. A. Ranter, *J. Phys. Chem. B* **108**, 8817 (2004).
 - [5] R. P. Sear, S. W. Chung, G. Markovich, W. M. Gelbart, and J. R. Heath, *Phys. Rev. E* **59**, R6255 (1999).
 - [6] R. Lipowsky, *Nature* **349**, 475 (1991); G. Ayton and G. A. Voth, *Biophys. J.* **83**, 3357 (2002).
 - [7] B. Widom, K. A. Dawson, and M. D. Lipkin, *Physica A* **140**, 26 (1986); K. A. Dawson, *Phys. Rev. A* **36**, 3383 (1987).
 - [8] J. Schmalian and P. G. Wolynes, *Phys. Rev. Lett.* **85**, 836 (2000); S. W. Wu, H. Westfahl Jr., J. Schmalian, and P. G. Wolynes, *Chem. Phys. Lett.* **359**, 1 (2002).
 - [9] E. J. W. Verwey and J. TH. G. Overbeek, *Theory of the Stability of Lyophobic Colloids*, (Elsevier, Amsterdam, 1948).
 - [10] C. Wu and S. H. Chen, *J. Chem. Phys.* **87**, 6199 (1987).
 - [11] F. Sciortino, S. Mossa, E. Zaccarelli, and P. Tartaglia, *Phys. Rev. Lett.* **93**, 055701 (2004); S. Mossa, F. Sciortino, P. Tartaglia, and E. Zaccarelli, *Langmuir* **20**, 10756 (2004); F. Sciortino,

- P. Tartaglia, and E. Zaccarelli, arXiv:cond-mat/0505453.
- [12] J. L. Wu, Y. Liu, W. R. Chen, J. S. Cao, and S. H. Chen, Phys. Rev. E **70**, 050401 (2004).
- [13] P. M. Chaikin, P. Pincus, S. Alexander, and D. Hone, J. Colloid and Inter. Sci. **89**, 555 (1982);
K. Kremer, M. O. Robbins, and G. S. Grest, Phys. Rev. Lett. **57**, 2694, (1986).
- [14] G. Malescio and G. Pellicane, Nat. Mater. **2**, 97 (2003).
- [15] J. L. Wu and J. S. Cao, accepted by J. Phys. Chem. B; A. Zhukov and J. S. Cao, In preparation.